Electronic Supplementary Material (ESI) for Journal of Materials Chemistry A.

Supporting Information

Polypyrrole indexing hollow metal-organic framework composites for lithium-sulfur batteries

Pengbiao Geng, Shuai Cao, Xiaotian Guo, Jiawei Ding, Songtao Zhang, Mingbo Zheng and Huan Pang

School of Chemistry and Chemical Engineering, Guangling College,
Yangzhou University, Yangzhou, 225009, Jiangsu, P. R. China.
E-mail: huanpangchem@hotmail.com, panghuan@yzu.edu.cn

Table of Contents

Experiment

Synthesis of ZIF-67: ZIF-67 was synthesized according to a common method: 0.616 g 2-methylimidazole (2-HmIm) and 0.546 g $Co(NO_3)_2 \cdot 6H_2O$ dissolved in 15 mL CH_3OH respectively. The 2-HmIm solution was slowly added in $Co(NO_3)_2 \cdot 6H_2O$ solution and the mixed solution was sonicated in an ultrasonic cleaner for 15 minutes. Then the purple product was separated by centrifugation and washed 3 times with methanol. After that, the product was dried under vacuum at 60 °C for 16 h to remove the residual methanol for the entrance of sulfur in the next step.

Synthesis of ZIF-67-S: Sublimed sulfur were successfully introduced into pores of ZIF-67 in a quantitative manner through melt diffusion at 130 °C. Taking ZIF-67-S with 50 wt.% sublimed sulfur loading (ZIF-67-S-50%) as an example, 150 mg of ZIF-67 powder was firstly grinded together with 150 mg of sublimed sulfur to get a fine mixture. The mixture was transferred into a 50-mL Teflon-line sealed autoclave and heated at 130 °C for 800 min to generate the ZIF-67-S-50% sample.

Synthesis of ZIF-67-S-PPy: To prepare ZIF-67-S-PPy, we choose Fe^{3+} as oxidizing agent to motivate the polymerization of pyrrole monomer. 200 mg of ZIF-67-S particles were dispersed in 15 mL 0.4 M PVP aqueous solution via ultrasonic for 1 min. The resulting turbid suspension was stirred for 30 mins. In the same time, Fe^{3+} solution was prepared (0.9g $FeCl_3 \bullet 6H_2O$ + 10 mL deionized water). After centrifuging the above turbid suspension using deionized water for three times, stirred with pyrrole monomers in 15 ml deionized water for 10 mins, the prepared Fe^{3+} solution (pyrrole: Fe^{3+} =1:3 by molar ratio) was added and stirred in dark for 12 h at 0 °C. After reaction, the black precipitate was collected by centrifuging and washed repeatedly with deionized water and ethanol to remove pyrrole monomers and salt residue in the product. Finally, the precipitate was dried at 60 °C in vacuum for 12 h to

provide the final dry ZIF-67-S-PPy, labeling as ZIF-67-S-PPy-50%, -60% and -70% respectively.

Characterization

SEM images were obtained by Zeiss-Supra 55 microscope at an acceleration voltage of 5 kV. TEM images of the samples were obtained using a JEM-2100 microscope at an acceleration voltage of 200 kV. The PXRD patterns was performed by Bruker AXS D8 advance with Cu Kα radiation of 40 kV (λ=1.5418 Å). FT-IR measurement was investigated on a TENSOR27. The N_2 adsorption-desorption isothermals and pore size distribution were obtained by Autosorb-iQ via BET method. EDS elemental mapping scans were recorded using Tecnai G2 F30 S-TWIN at an acceleration voltage of 300 kV. XPS analysis was carried out using a Thermo Scientific ESCALAB 250Xi X-ray photoelectron spectrometer with Al Kα radiation of 1486.6 eV as the excitation source. The survey thickness is 2-3 nm.

Electrochemical Measurements

Electrode preparation of ZIF-67-S-PPy (-50%, -60% and -70%), ZIF-67-S and S-PPy: The slurry is mixed with sample powders, Super P and Polyvinylidene Fluoride (PVDF) in a weight ratio of 70 : 20 : 10 in N-methyl-2-pyrrolidone (NMP) as dispersant. Then the slurry is cast on the Al foil and dried overnight at 60 °C under vacuum condition. However, preparation of sulfur electrode is different from the above. To improve the electrical conductivity of sublimed sulfur, Super P was firstly grinded together with sublimed sulfur (weight ratio of Super P and sublimed sulfur = 80 : 20) and then transferred into a 50-mL Teflon-line sealed autoclave and heated at 130 °C for 800 min to generate the S-Super P. Then mixed with Super P and PVDF like the above method. The obtained working electrodes were cut to circular electrode with a diameter of 12 mm. The accurate sulfur mass on each electrode was calculated according to thermogravimetric analysis (TGA) curves under N_2 flow. The mass loading of active sulfur was 0.5~1.2 mg cm^{-2}. The CR 2032-type coin cells were fabricated using the working

electrode, Lithium foil as the counter and anode electrode, Celgard 2400 as the separator. The electrolyte was used 1.0 M lithium bis(trifluoromethanesulfonyl)imide (LiTFSI Sigma-Aldrich (USA), 99.95%) in 1, 3-dioxolane (DOL, Sigma-Aldrich (USA), 99.0%) and 1, 2-dimethoxyethane (DME, Junsei (Japan), 99.0%) (volume ratio, 1:1). 35 µL of electrolyte was used in the fabrication of each Li-S cell in an argon-filled glove box (where both water and oxygen levels are below 10^{-7}. The other four samples were also fabricated cells in same way. The GCD tests were estimated in the voltage window of 1.7-2.7 V. The rate capability was also tested by varying the current density from 0.1C to 1C (1 C = 1675 mA g^{-1}) on a battery measurement system (CT2001A, Wuhan Land, China) at room temperature. CV and EIS curves were measured on an electrochemical workstation (CHI660E, Chenhua, Shanghai, China).

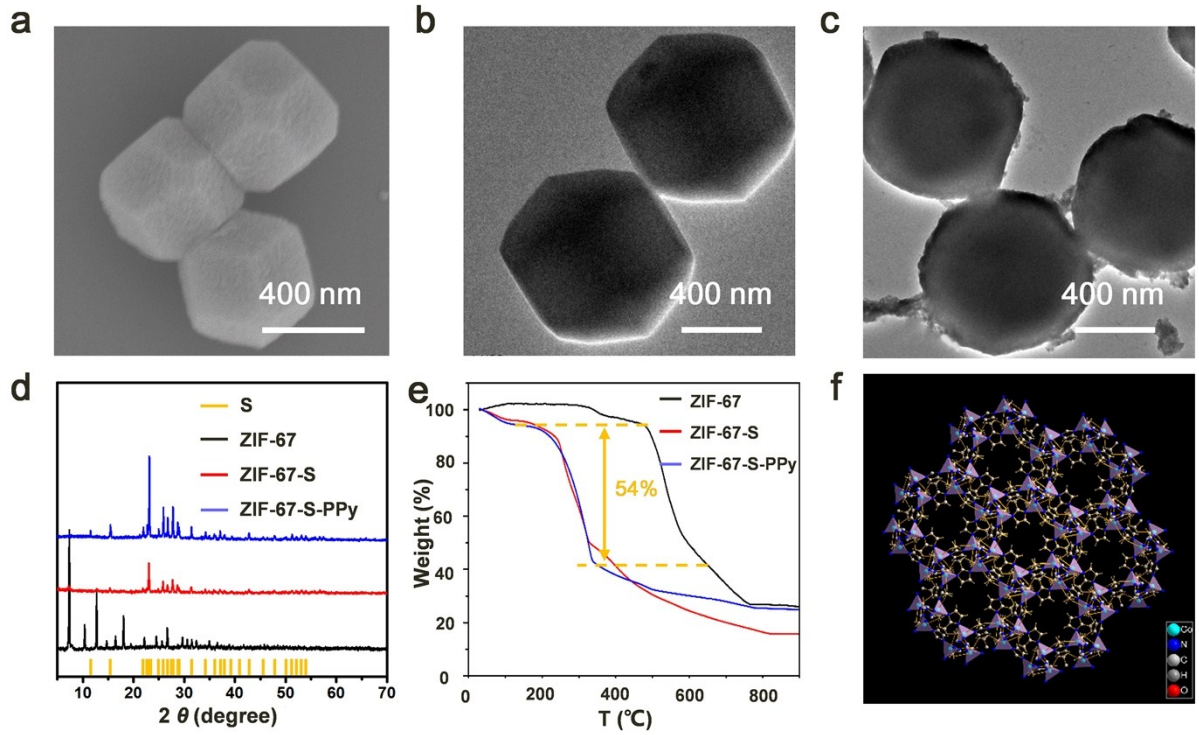

Figure S1. a) SEM image of ZIF-67. b) TEM image of ZIF-67-60%. c) TEM image of ZIF-67-S-PPy-60%. d) XRD pattern of ZIF-67, ZIF-67-60% and ZIF-67-S-PPy-60%. e) TGA curve of ZIF-67, ZIF-67-S-60% and ZIF-67-S-PPy-60%. f) Secondary building unit (SBU) and organic linker of ZIF-67.

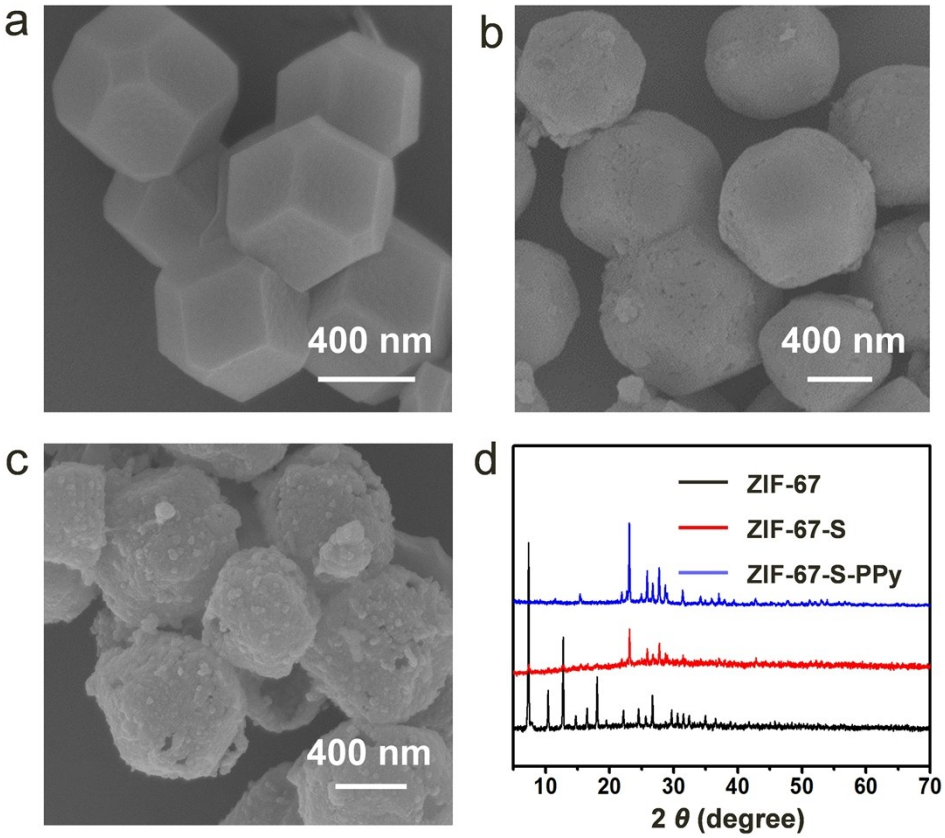

Figure S2. a, b and c) SEM images of ZIF-67, ZIF-67-S-50% and ZIF-67-S-PPy-50%; d: XRD patterns of ZIF-67, ZIF-67-S-50% and ZIF-67-S-PPy-50%.

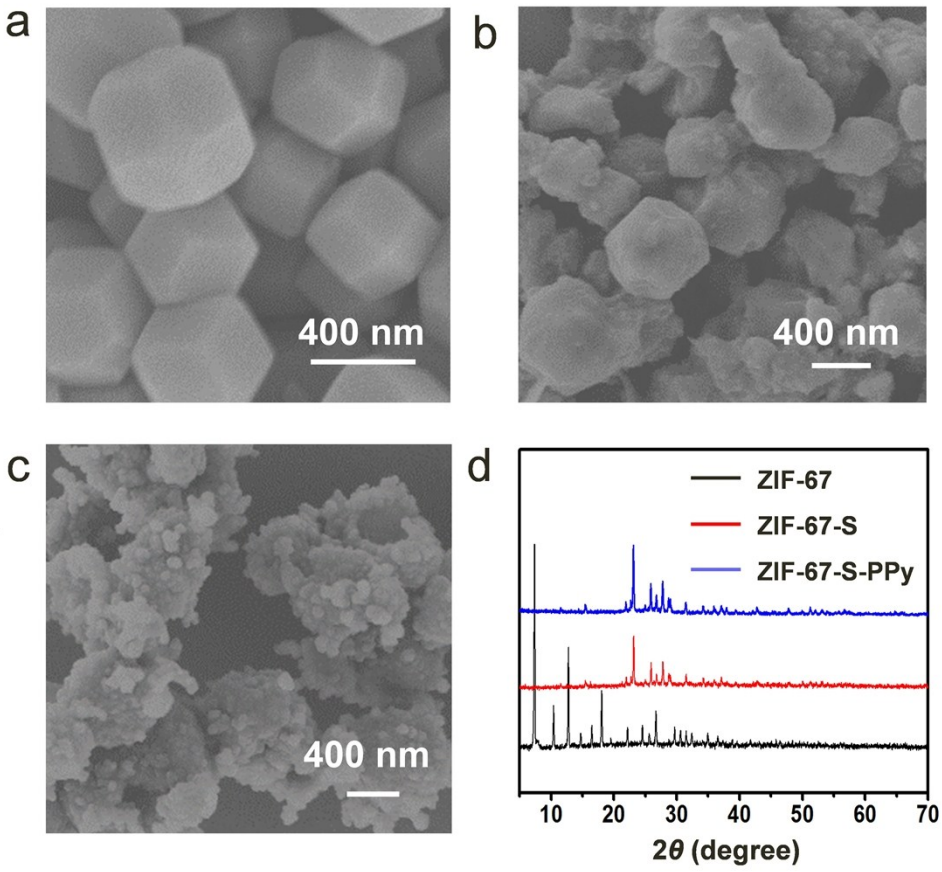

Figure S3. a, b and c) SEM images of ZIF-67, ZIF-67-S-70% and ZIF-67-S-PPy-70%; d: XRD patterns of ZIF-67, ZIF-67-S-70% and ZIF-67-S-PPy-70%.

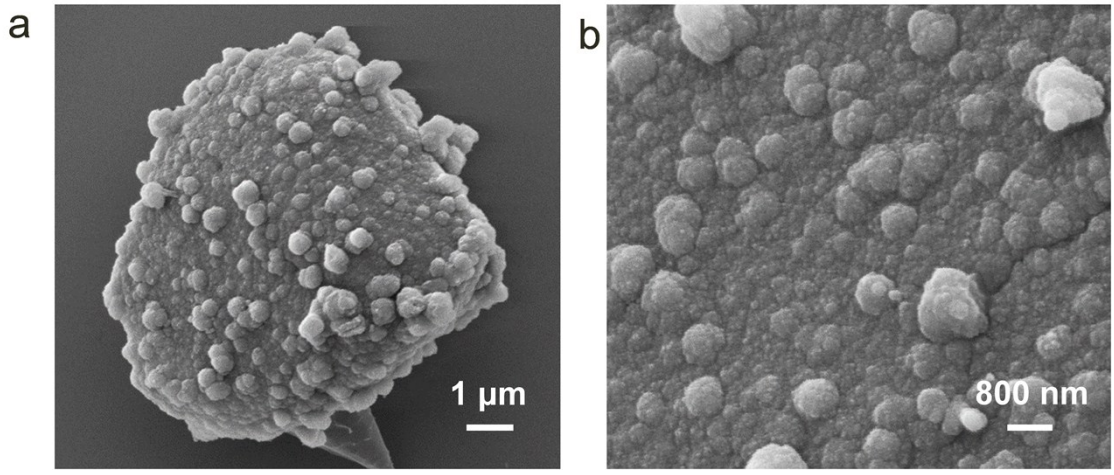

Figure S4. a and b) SEM images of S-PPy

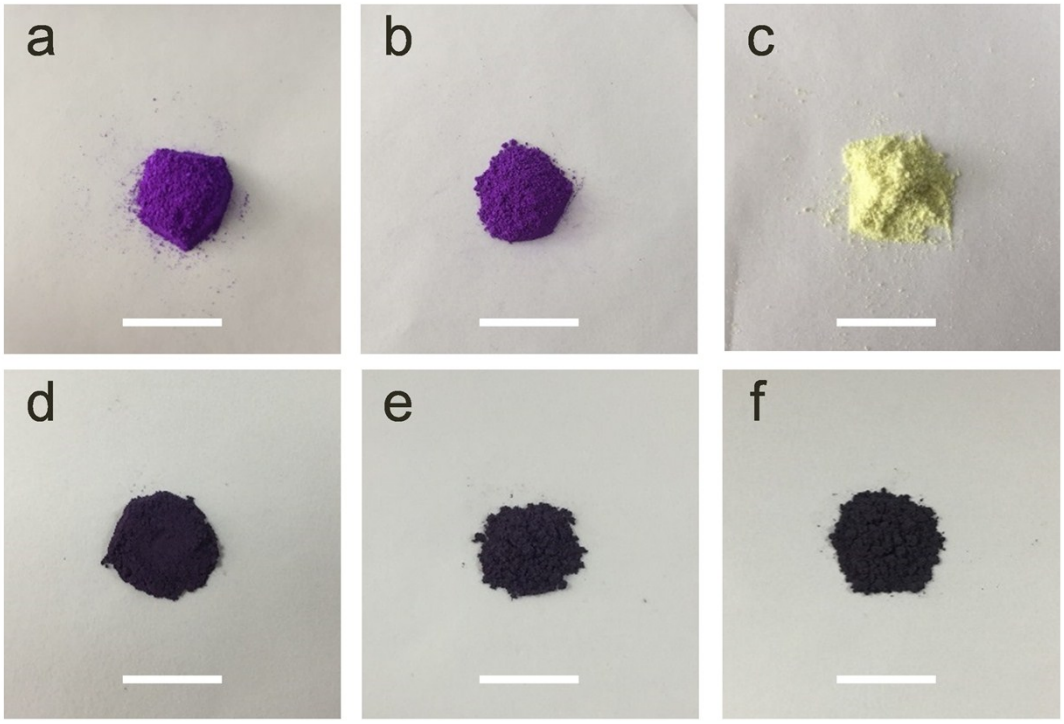

Figure S5. Optical images of ZIF-67, ZIF-67-130 ℃, S-130 ℃, ZIF-67-S-50%, ZIF-67-S-60% and ZIF-67-S-70% respectively, scale bar is 1cm.

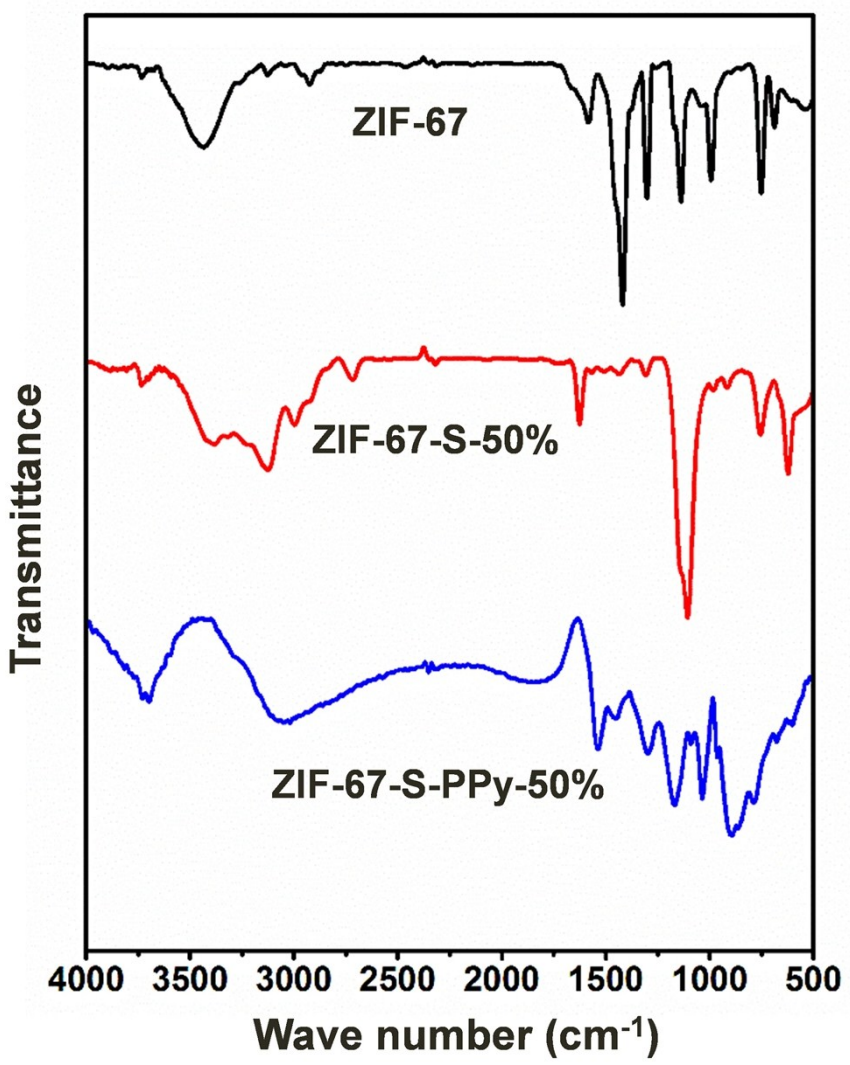

Figure S6. FT-IR spectrum of ZIF-67, ZIF-67-S-50% and ZIF-67-S-PPy-50%.

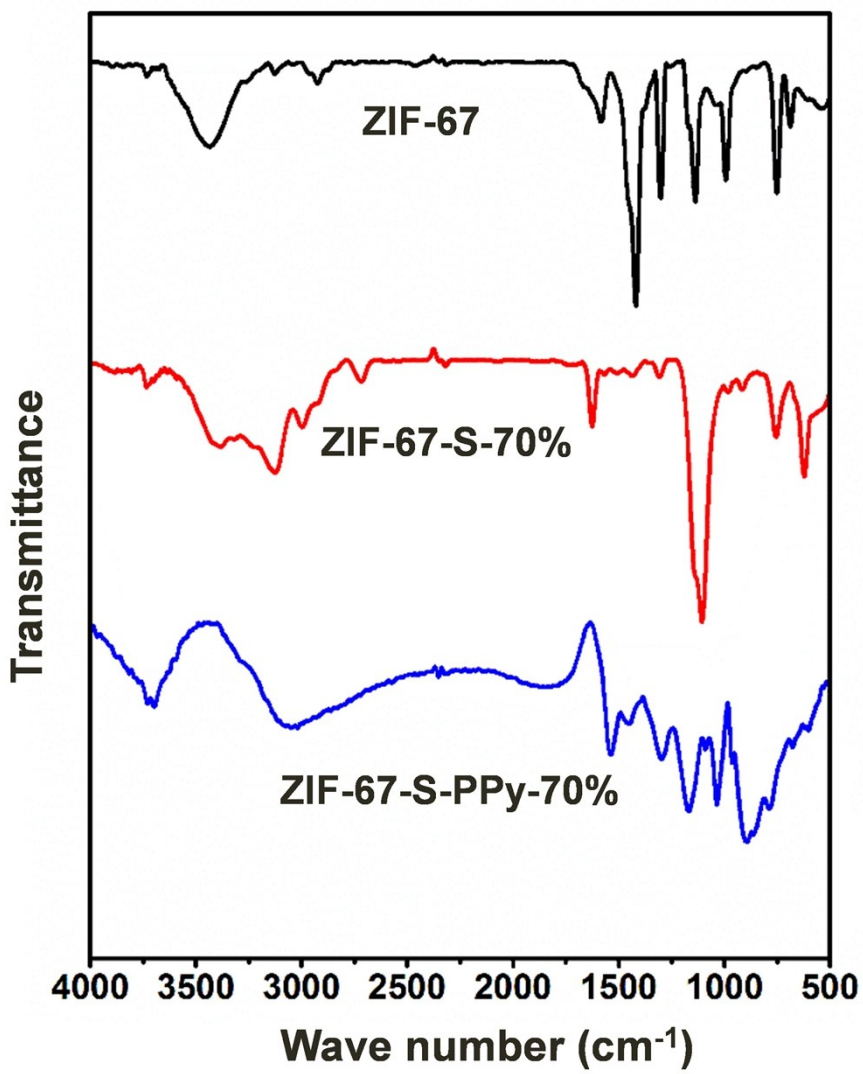

Figure S7. FT-IR spectrum of ZIF-67, ZIF-67-S-70% and ZIF-67-S-PPy-70%.

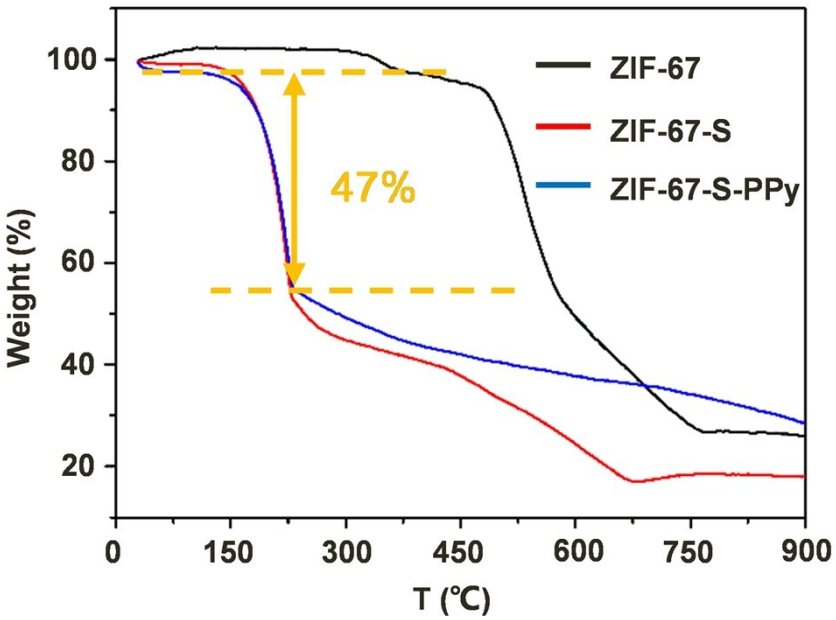

Figure S8. TGA curves of ZIF-67, ZIF-67-S-50%, ZIF-67-S-PPy-50%.

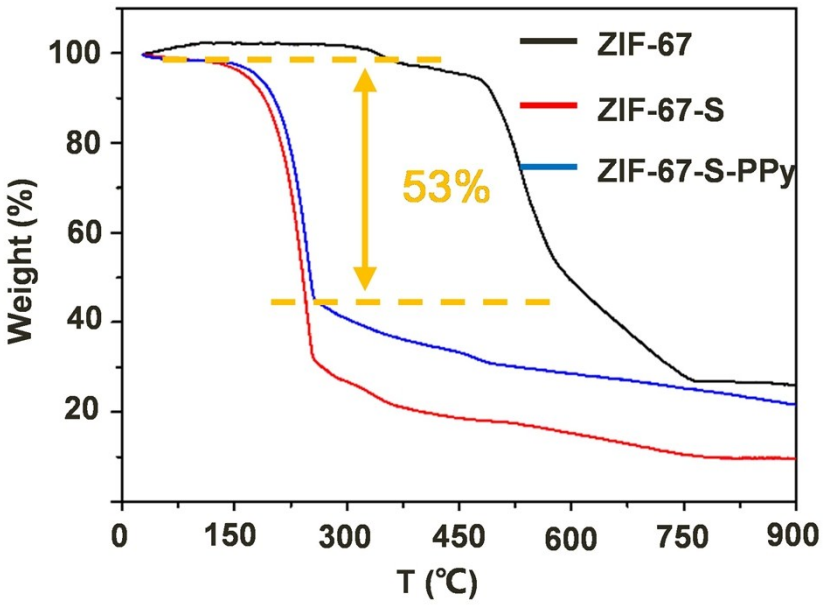

Figure S9. TGA curves of ZIF-67, ZIF-67-S-70%, ZIF-67-S-PPy-70%.

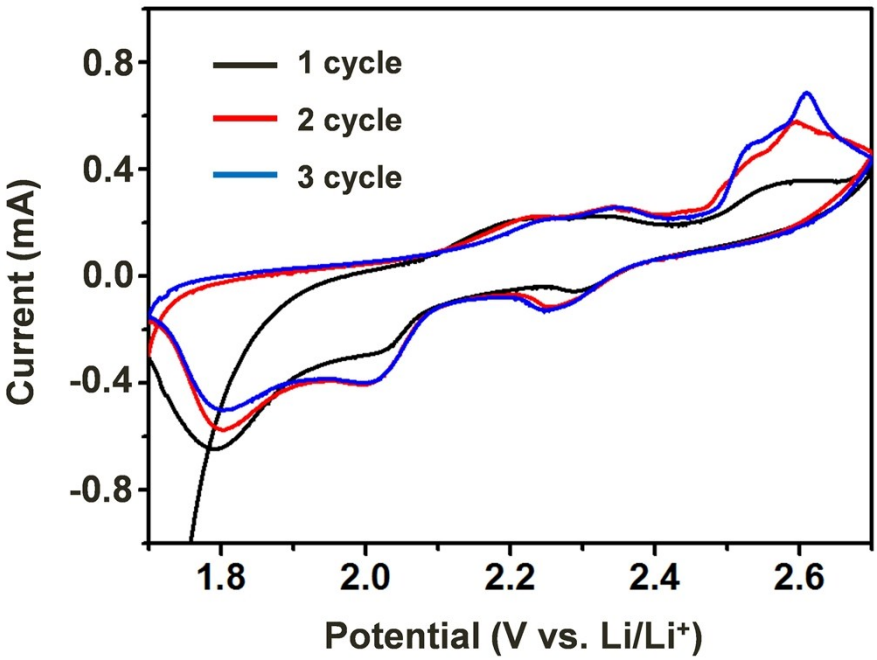

Figure S10. CV curves of initial three cycles of ZIF-67-S-60% electrode at a scan rate of 0.5 mV s^{-1}.

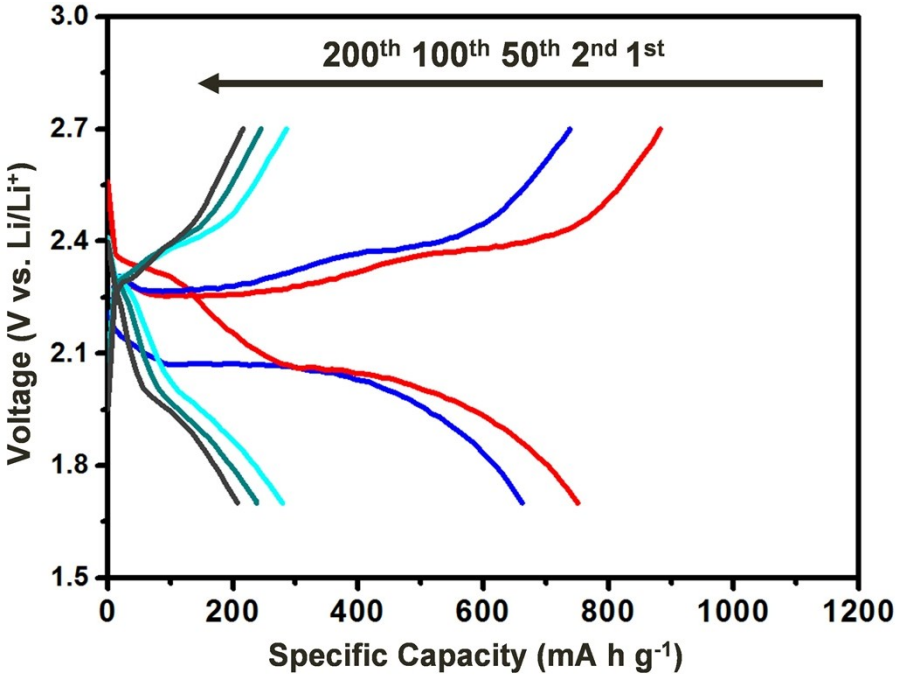

Figure S11. The GCD voltage profiles of ZIF-67-S-PPy-50%.

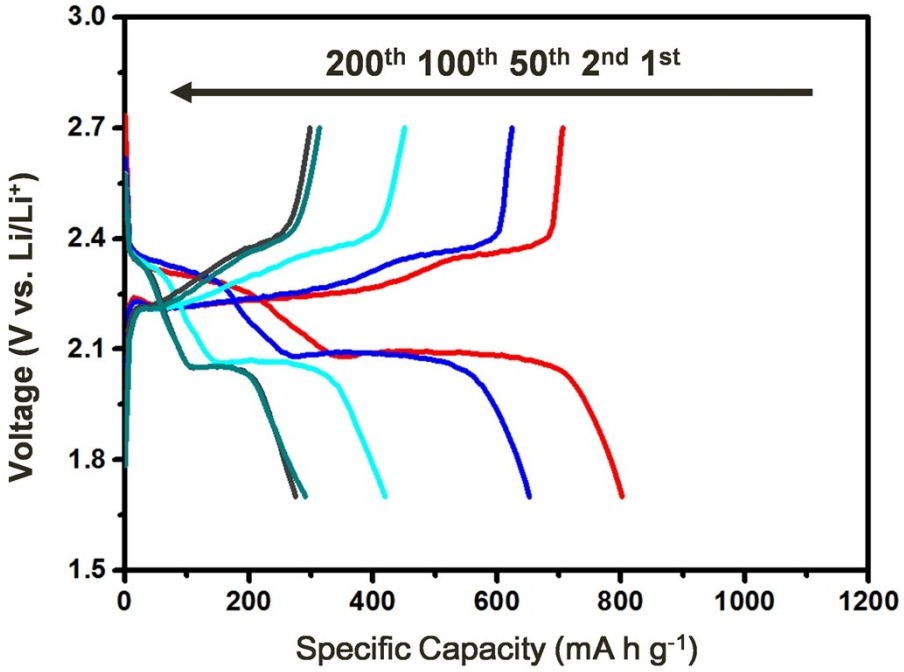

Figure S12. The GCD voltage profiles of ZIF-67-S-PPy-70%.

Table S1. Comparison of the specific capacity for reported sulfur host.

Host Materials	Initial Capacity ($mAh\ g^{-1}$)	Cycles Number	Final Capacity ($mAh\ g^{-1}$)	Discharge Rate	References
ZIF-8	950	250	712.5	0.5C	1
ZIF-67	255	1000	155	0.2C	2
$[(CH_3)_2NH_2]_2[Cd(L)]\cdot 5DMF$	1092	50	799	0.1C	3
NC-Se-50	980	200	443.2	0.5C	4
Ni-MOF	686.5	100	611	0.1C	5
HKUST-1	1498	170	500	0.1C	6
$Na_2Fe[Fe(CN)_6]$@PEDOT	819	100	770	2C	7
CTF-1	562	300	482.2	1C	8
MIL-53-PPy	793	300	347	0.5C	9
S@Cu-TDPAT	820	500	745	1C	10
nMOF-867	870	500	680	835 $mA\ g^{-1}$	11
MOF-525(2H)	1180	200	402	0.5C	12
MOF-525(FeCl)	1195	200	616	0.5C	12
MOF-525(Cu)	998	200	704	0.5C	12
GNS-MIL-101(Cr)	497	300	396.9	2.4C	13
GNS-MIL-101(Cr)	1263	500	680	0.2C	14
ZIF-67-S-PPy	**1092.5**	**200**	**353.6**	**0.1C**	**This work**

References:

1 J. Zhou, X. Yu, X. Fan, X. Wang, H. Li, Y. Zhang, W. Li, J. Zheng, B. Wang and X. Li, *J. Mater. Chem. A*, 2015, **3**, 8272–8275.

2 L. Bai, D. Chao, P. Xing, L. Tou, Z. Chen, A. Jana, Z. Shen and Y. Zhao, *ACS Appl. Mater. Interfaces*, 2016, **8**, 14328–14333.

3 M. Li, Y. Sun, K. Zhao, Z. Wang, X. Wang, Z. Su and H. Xie, *ACS Appl. Mater. Interfaces*, 2016, **8**, 33183–33188.

4 Z. Li and L. Yin, *Nanoscale*, 2015, **7**, 9597–9606.

5 J. Zheng, J. Tian, D. Wu, M. Gu, W. Xu, C. Wang, F. Gao, M. H. Engelhard, J.-G. Zhang, J. Liu and J. Xiao, *Nano Lett.*, 2014, **14**, 2345–2352.

6 Z. Wang, X. Li, Y. Cui, Y. Yang, H. Pan, Z. Wang, C. Wu, B. Chen and G. Qian, *Cryst. Growth Des.*, 2013, **13**, 5116–5120.

7 D. Su, M. Cortie, H. Fan and G. Wang, *Adv. Mater.*, 2017, **29**, 1700587.

8 S. Talapaneni, T. Hwang, S. Je, O. Buyukcakir, J. Choi and A. Coskun, *Angew. Chem. Int. Ed.*, 2016, **55**, 3106–3111.

9 J. Zhou, R. Li, X. Fan, Y. Chen, R. Han, W. Li, J. Zheng, B. Wang and X. Li, *Energy Environ. Sci.*, 2014, **7**, 2715.

10 X. Hong, T. Tan, Y. Guo, X. Tang, J. Wang, W. Qin and Y. Cai, Nanoscale, 2018, 10, 2774–2780.

11 J. Park, K. Choi, D. Lee, B. Moon, S. Shin, M. Song and J. Kang, Sci. Rep., 2016, 6, 25555.

12 Z. Wang, B. Wang, Y. Yang, Y. Cui, Z. Wang, B. Chen and G. Qian, ACS Appl. Mater. Interfaces, 2015, 7, 20999–21004.

13 Z. Zhao, S. Wang, R. Liang, Z. Li, Z. Shi and G. Chen, J. Mater. Chem. A, 2014, 2, 13509–13512.

14 Y. Mao, G. Li, Y. Guo, Z. Li, C. Liang, X. Peng and Z. Lin, Nat. Commun., 2017, 8, 14628.